

# Nitrogen Activation via Three-Coordinate Molybdenum Complexes: Comparison of Density Functional Theory Performance with Wave Function Based Methods

David C. Graham,<sup>†</sup> Gregory J. O. Beran,<sup>§</sup> Martin Head-Gordon,<sup>§</sup> Gemma Christian,<sup>‡</sup> Robert Stranger,<sup>‡</sup> and Brian F. Yates<sup>\*,†</sup>

School of Chemistry, University of Tasmania, Private Bag 75, Hobart, Tasmania 7001, Australia, Department of Chemistry, University of California, and Chemical Sciences Division, Lawrence Berkeley National Laboratory, Berkeley, California 94720, Department of Chemistry, The Australian National University, Canberra ACT 0200, Australia

Received: December 20, 2004; In Final Form: May 31, 2005

Obtaining an accurate theoretical model for the activation of dinitrogen by three-coordinate molybdenum amide complexes (e.g. Mo(NH<sub>2</sub>)<sub>3</sub>) is difficult due to the interaction of various high- and low-spin open-shell complexes along the reaction coordinate which must be treated with comparable levels of accuracy in order to obtain reasonable potential energy surfaces. Density functional theory with present-day functionals is a popular choice in this situation; however, the dinitrogen activation reaction energetics vary substantially with the choice of functional. An assessment of the reaction using specialized wave function based methods indicates that although current density functionals in general agree qualitatively on the mechanistic details of the reaction, a variety of high-level electron correlation methods (including CCSD(T), OD(T), CCSD(2), KS-CCSD(T), and spin-flip CCSD) provide a consistent but slightly different representation of the system.

## Introduction

Activation of dinitrogen (N<sub>2</sub>) represents a difficult synthetic challenge given the strong nature of the nitrogen triple bond.<sup>1–3</sup> Significant attention has focused on the use of transition metals in this process, with the aim of achieving activation under relatively mild conditions.<sup>4–10</sup> In 1995, Laplaza and Cummins described<sup>11</sup> the experimental cleavage of dinitrogen by a sterically hindered three-coordinate Mo(III) complex, Mo[N(R)Ar]<sub>3</sub> (R = C(CD<sub>3</sub>)<sub>2</sub>CH<sub>3</sub>, Ar = 3,5-C<sub>6</sub>H<sub>3</sub>Me<sub>2</sub>),<sup>12</sup> resulting in the formation of a terminal nitrido Mo(VI) product (Figure 1).<sup>11,13,14</sup>

The reactant, intermediate, and products from the reaction have been characterized using a variety of experimental methods. The reactant has been isolated and its structure determined by X-ray crystallography,<sup>15</sup> with SQUID magnetic susceptibility measurements consistent with a quartet electronic state ( $\mu_{\text{eff}} = 3.87 \mu_{\text{B}}$ ).<sup>13</sup> Obtaining crystals of the thermally unstable intermediate ( $\mu\text{-N}_2$ ){Mo[N(R)Ar]<sub>3</sub>}<sub>2</sub> proved difficult, but EXAFS measurements on a -35 °C toluene solution of the compound suggest an essentially linear MoNNMo core, with an N–N bond length of 1.19 Å.<sup>16</sup> Magnetic susceptibility measurements on the closely related phenyl analogue (( $\mu\text{-N}_2$ ){Mo[N(R)Ph]<sub>3</sub>}<sub>2</sub>) are indicative of a triplet ground state for the intermediate ( $\mu_{\text{eff}} = 2.85 \mu_{\text{B}}$ ).<sup>13</sup> Synthesis of the phenyl analogue of the diamagnetic product (NMo[N(R)Ph]<sub>3</sub>) has also resulted in X-ray-quality crystals suitable for structural analysis.<sup>13</sup> Using variable-temperature kinetic studies, the activation barrier required for nitrogen scission from the intermediate was estimated to be approximately 97 kJ mol<sup>-1</sup>.<sup>13</sup>

A number of theoretical studies<sup>17–24</sup> have emerged detailing the cleavage of the N≡N triple bond of both N<sub>2</sub> and N<sub>2</sub>O.<sup>15,25</sup>

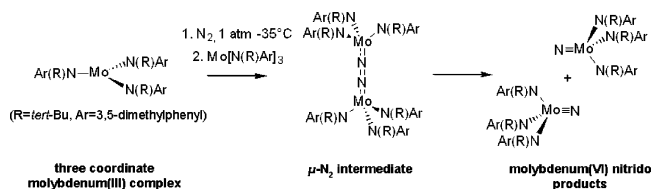


**Figure 1.** Activation of dinitrogen using a sterically hindered three-coordinate molybdenum complex.

by three-coordinate molybdenum complexes. Apart from a molecular mechanics investigation by Rösch and co-workers,<sup>19</sup> those studies describing nitrogen activation have opted for a simplified model system rather than the experimental full-ligand system. The initial theoretical study of the nitrogen activation reaction was performed by Cui et al.,<sup>17</sup> who characterized the species on the proposed potential energy surface using density functional theory (DFT) calculations on a model system (Mo(NH<sub>2</sub>)<sub>3</sub>). Morokuma's group proposed that the reaction proceeded by easy formation of a quartet encounter complex through end-on coordination of N<sub>2</sub> to the quartet reactant, which on coupling with an additional reactant molecule gives the triplet intermediate via a nonadiabatic process. Spin crossover from the intermediate through a singlet zigzag transition structure then furnishes the resultant nitrido products (Figure 2). Remarkably, prediction of the triplet ground state for the intermediate and an accurate estimation of  $E_{\text{act}}$  (87 kJ mol<sup>-1</sup>) were achieved, even before experimental evidence was available.<sup>13</sup>

Further investigations by other researchers on the reaction using the same model system have revealed discrepancies between their work and that of the Morokuma group. A study by Neyman et al.,<sup>18</sup> stressing the importance of relativistic effects for accurate calculation of the activation barrier and reaction enthalpy, noted that while the geometries of reactants and products obtained were in perfect agreement with those of the

\* To whom correspondence should be addressed. E-mail: Brian.Yates@utas.edu.au.

<sup>†</sup> University of Tasmania.

<sup>§</sup> University of California and Lawrence Berkeley National Laboratory.

<sup>‡</sup> The Australian National University.

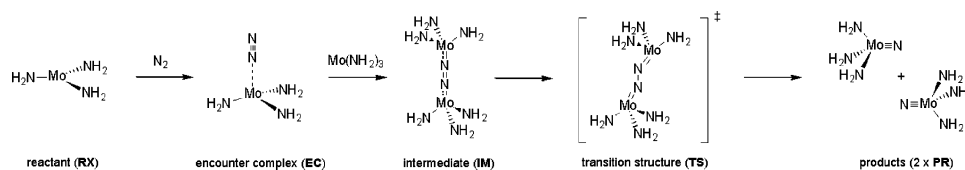


**Figure 2.** Characterized species on the nitrogen activation pathway using DFT on a model complex (Mo(NH<sub>2</sub>)<sub>3</sub>).

Morokuma group, the reaction enthalpy differed by ca. 80 kJ mol<sup>-1</sup>. More recently, Christian et al.<sup>23</sup> demonstrated the existence of an alternate singlet intermediate which was stabilized by rotation of an amide group at each metal center, resulting in a structure lying 14 kJ mol<sup>-1</sup> below the linear triplet intermediate located by the Morokuma group. This result, while inconsistent with experimental observations on (μ-N<sub>2</sub>){Mo-[N(R)Ph]<sub>3</sub>}<sub>2</sub>, does rely on ligand rotation, a process that may be restricted in the full ligand system.<sup>24</sup>

While all these investigations relied on density functional theory, the choice of gradient-corrected functional differed in the more recent studies. In general, the functionals chosen to study this system (i.e. B3LYP<sup>26–28</sup> and BP<sup>27,29</sup>) have shown excellent predictive ability when applied to transition metal complexes,<sup>30–35</sup> although difficulties have been known to occur with calculations involving both low- and high-spin configurations of open-shell transition metals,<sup>36–42</sup> as is the case here. Attempts by Hess and co-workers<sup>36</sup> to predict known low- and high-spin configurations of experimentally isolable Fe(II) complexes saw differences of up to 100 kJ mol<sup>-1</sup> between functionals. In this case, reparametrization of B3LYP (referred to as B3LYP\*) was carried out in order to obtain results conforming to the experimentally observed electronic states.<sup>36,43</sup>

This paper details the comparison of popular density functional methods with wave function based methods in an effort to accurately represent the potential energy surface for the activation of nitrogen by three-coordinate molybdenum amide complexes. At present, there is some discussion about the nature of the reaction path, with uncertainty surrounding the electronic state of the intermediate. A proper understanding of the mechanism through accurate characterization of electronic states for each of the species along the pathway is essential before the development of more active theoretical and, ultimately, experimental systems can be achieved.

## Methods

A major difficulty with the ab initio study of open-shell systems in general and transition metals in particular is the inadequacy of the elementary Hartree–Fock (HF) model chemistry to provide a reasonable basic description of the system. The HF wave function will tend to break both spatial and spin symmetry as it tries to describe the multiconfigurational wave function within the confines of a single determinant.<sup>44–48</sup> Density functional theory with present-day functionals tends to behave better in terms of symmetry breaking,<sup>49,50</sup> though, as previously mentioned, the functionals are not necessarily well-designed for transition metal properties in systems with both low- and high-spin configurations.<sup>36,43</sup> The advantage of wave function based methods is that the model can be methodically improved.<sup>51–53</sup> Unfortunately, these methods are inherently tied to the HF reference wave function. In systems with complicated electronic structure like transition metal complexes for which HF provides a poor reference (due to symmetry-breaking effects, for example), these methods (particularly the perturbative ones) become highly suspect.<sup>44,47,48</sup> With problems such as this in

mind, some recently developed coupled cluster methods have attempted to break this link to HF theory.

In traditional CCSD, the single and double excitations are defined in terms of the HF molecular orbitals. In cases where HF lacks the flexibility to provide even a qualitative description of the system, it would be preferable to reoptimize the orbitals such that they minimize the coupled cluster (CC) energy. This approach is known as orbital-optimized coupled cluster doubles, or simply optimized doubles (OD).<sup>54</sup> This orbital optimization plays a similar role to the single excitations in CCSD (which are usually attributed to orbital relaxation effects), so the inclusion of singles is unnecessary. The method is similar to the Brueckner coupled cluster doubles method.<sup>55</sup> Computationally, OD and CCSD scale the same formally, but the repeated orbital optimization steps mean that frequent change of bases to the updated molecular orbitals are necessary, so in practice OD costs a factor of a few more than CCSD. The primary benefit of OD over CCSD is that often the symmetry-breaking in the HF reference is substantially reduced.<sup>54</sup> Although this does not often change the energetics relative to CCSD significantly, the results of OD(T) calculations can be dramatically improved over those from CCSD(T). For example, the vibrational frequency of doublet NO radical changes from 216 cm<sup>-1</sup> too large as compared to experiment with CCSD(T) to only 5 cm<sup>-1</sup> too small with OD(T) in the cc-pVTZ basis.<sup>56</sup>

Unfortunately, OD is currently computationally unaffordable for the largest species in this system (**1TS**, **1IM**, and **3IM**). Therefore, we also utilize the low-cost alternative to OD(T) demonstrated in ref 56, in which HF orbitals in a standard CCSD(T) calculation are replaced by Kohn–Sham (KS) orbitals from a DFT calculation to obtain accurate OD(T)-like results at CCSD(T) cost. This is termed KS-CCSD(T), and we have applied this method with both B3LYP and BP86 reference orbitals.

For higher order correlation effects (i.e. beyond double excitations), we use two distinct noniterative perturbative corrections. The first is the widely used (T) correction to account for triple excitations.<sup>53</sup> Second, we use the (2) correction proposed by Gwaltney and Head-Gordon, which accounts for the effects of triple and quadruple excitations.<sup>57,58</sup> The (T) correction is fundamentally based on the HF reference, as it was developed by comparing terms in fifth-order Møller–Plesset perturbation theory with those found in CCSD. The (2) correction, on the other hand, takes as its zero-order Hamiltonian the space in which we have solved the CC equations (e.g. CCSD or OD) and computes the second-order correction for the remaining unsolved space. This means that the zero-order energy is CCSD (or OD) rather than the HF energy. Because CCSD and OD are much more robust than HF, the (2) correction tends to resist perturbative breakdowns for difficult problems such as bond-stretching, etc. The (2) correction typically requires 3–5 times the computational effort of (T).

The other inherent difficulty in this system is the mixture of species of different spin states along the potential energy surface. The theoretical model must be able to treat both high-spin species and open-shell low-spin electronic configurations, which

can be highly multiconfigurational, with comparable accuracy. A poor treatment of the open-shell low-spin species' electronic structure will result in an energy that is too high. When comparing the low-spin species against the more easily described high-spin species, the errors will manifest themselves prominently. We must therefore establish the validity of the single reference model used for these species.

Traditionally, one would verify the standard coupled cluster results by carefully choosing configurations in a multireference configuration interaction-like method. Instead, we use spin-flip CCSD (SF-CCSD) developed by Krylov and Levchenko.<sup>59,60</sup> In this single-reference approach, the low-spin open-shell states are described as excitations from the high-spin system involving a spin-flip. For example, a singlet state can be accessed from a triplet state by flipping one electron spin. The high-spin system is generally well-described by the single-reference method. Therefore, by generating the low-spin states in this manner, all the important configurations are generated in a balanced way. This approach is particularly useful for calculating singlet–triplet or doublet–quartet gaps,<sup>61</sup> and we will use it to validate our other CC approaches. In practice these computations are very similar to an equation of motion CCSD (EOM-CCSD) calculation and cost several times more than an ordinary CCSD calculation.

In this study, these advanced but somewhat costly coupled cluster methods will be used to validate other, more common and affordable procedures such as CCSD(T) and DFT with various functionals which can be used in more elaborate models for the system. Most calculations were carried out using the Gaussian03 suite of programs,<sup>62</sup> except for those calculations involving specialized electron-correlation methods (OD, OD(T), OD(2), KS-CCSD(T), SF-CCSD, and CCSD(2)) which were performed using Q-Chem version 2.1.<sup>63</sup>

## Results and Discussion

**Basis Set Effects.** Calculations to replicate the results of Cui et al.<sup>17</sup> (Figure 2) using the UB3LYP/LANL2DZ<sup>26–28,64,65</sup> model chemistry produced the set of geometries shown in parentheses in Figure 3. The nomenclature used (NXX) for the species on the pathway refers to the spin (N) where **1** = singlet and **2** = doublet, etc., and the position on the pathway (XX), where, for example, **TS** = transition structure. Optimized geometries are essentially identical to those obtained by the Morokuma group with several notable exceptions. The Mo–N<sub>2</sub> bond length is ca. 0.3 Å shorter in **4EC**, which is a product of a very flat potential energy surface in the Mo–N<sub>2</sub> = 2.5–3.5 Å region. The lowest energy structure of the singlet intermediate (**1IM**) was found to be a C<sub>2h</sub> symmetric species with a rotated amide group at each of the molybdenum centers, a result consistent with the recent results of Stranger et al.<sup>23</sup> Additionally, while a C<sub>2h</sub> transition structure geometry analogous to that of the Morokuma group was located, rotation of one of the molybdenum centers resulted in a lower energy conformer (**1TS**) containing a significantly less activated dinitrogen bond (1.480 cf. 1.544 Å). Consistent with the geometric differences observed for the species on the reaction pathway, the potential energy surface also changes slightly with respect to that calculated by the Morokuma group (Figure 4). The energy of the rotated amide singlet intermediate is lowered by ca. 22 kJ mol<sup>-1</sup> to –220.4 kJ mol<sup>-1</sup>, remaining slightly higher in energy than the analogous triplet (–225.1 kJ mol<sup>-1</sup>). Similarly, the lower energy conformer located for the C<sub>2h</sub> transition structure is lower in energy by ca. 12 kJ mol<sup>-1</sup>, thus reducing the calculated activation energy for dinitrogen cleavage from 87<sup>17</sup> to 75 kJ mol<sup>-1</sup>.

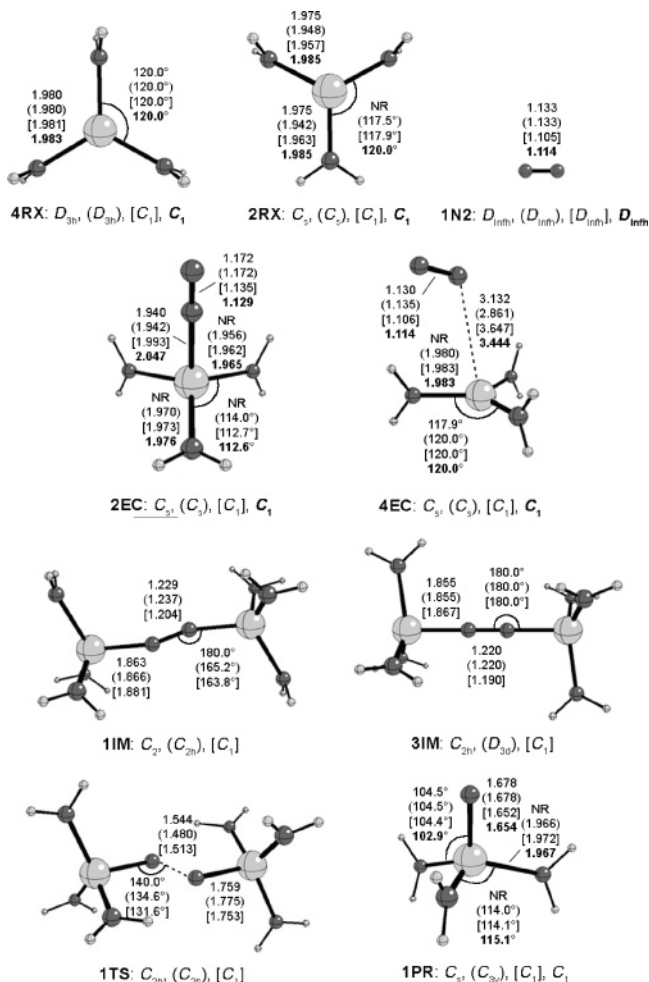


**Figure 3.** Optimized geometries for species on the reaction pathway shown in Figure 2. Values are in angstroms and degrees for the UB3LYP/LANL2DZ (Morokuma,<sup>17</sup> NR = not reported), (UB3LYP/LANL2DZ) (this study), [UB3LYP/GBS(I)], and **UCCSD/GBS(I)** levels of theory.

Reoptimization of all species was undertaken using UB3LYP and a compound general basis set, hereafter referred to as GBS(I), which included the LANL2DZ basis set<sup>64,65</sup> incorporating the Hay and Wadt effective core potential on molybdenum and the 6-31G(d) basis set<sup>66</sup> on all other atoms. To ensure accurate representation of the species on the reaction pathway, these optimizations were performed without symmetry constraints, using tight optimization criteria and an ultrafine grid.

In general, there are only subtle differences between the new geometries and those previously optimized at B3LYP/LANL2DZ (Figure 3). Relaxation of symmetry constraints identified an alternate geometry for the triplet intermediate (**3IM\***, Figure 5), which consists of an approximately linear core with significantly elongated Mo–N<sub>2</sub> bonds (1.903 Å) when compared to the **3IM** and **1IM** geometries calculated at GBS(I). While the pseudo-*S*<sub>6</sub> triplet intermediate (**3IM**) can be described geometrically as dinitrogen trapped between two of the quartet reactants (**4RX**), the extremities of the alternate triplet (**3IM\***) are reminiscent of the doublet reactant geometry that contains a rotated amide group.

With reference to the corresponding GBS(I) potential energy surface (in brackets, Figure 4), there are very marked differences with respect to the analogous surface obtained using LANL2DZ. In general, the exothermicity of all species on the surface is reduced somewhat in comparison to the LANL2DZ results. Destabilization of the products with respect to reactants results



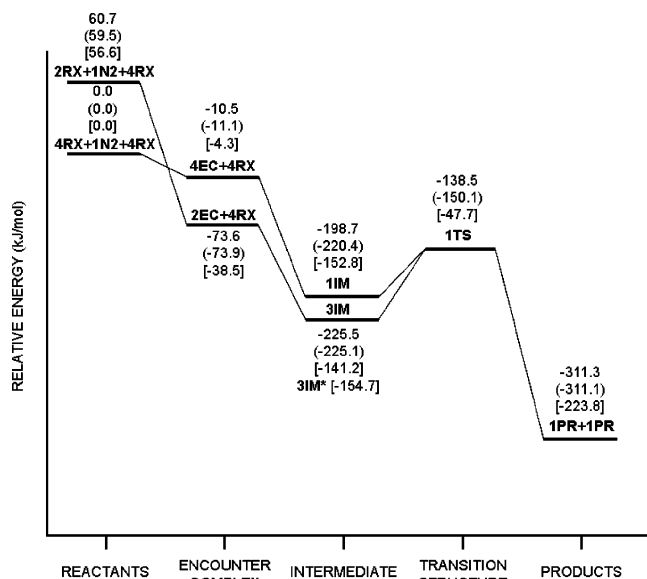


**Figure 4.** Variation of the dinitrogen activation PES with basis set. Relative energies are in kilojoules per mole and correspond to the UB3LYP/LANL2DZ (Morokuma<sup>17</sup>), (UB3LYP/LANL2DZ) (this study), and [UB3LYP/GBS(I)] levels of theory.

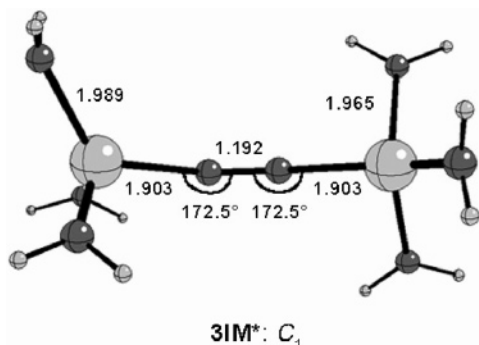


**Figure 5.** Alternate  $C_1$  geometry located for the triplet intermediate ( $3IM^*$ ) at the UB3LYP/GBS(I) level of theory.

in a decrease in the enthalpy of reaction by 87 kJ mol<sup>-1</sup> (to -223.8 kJ mol<sup>-1</sup>). Such a large effect on going from LANL2DZ to GBS(I) may well be due to the addition of d-type basis functions to the nitrogen atoms. While both spin states of the intermediate are somewhat higher in energy, the triplet intermediate ( $3IM$ ) is destabilized to a greater extent than the singlet ( $1IM$ ), such that the singlet now lies 11.6 kJ mol<sup>-1</sup> lower in energy than the triplet. Furthermore, relaxation of the pseudo- $S_6$  geometry of the triplet intermediate ( $3IM$ ) to  $C_1$  ( $3IM^*$ ) corresponds to a stabilization of 13.5 kJ mol<sup>-1</sup> on the UB3LYP/GBS(I) potential energy surface. Consequently, this stabilization places the alternate triplet 1.9 kJ mol<sup>-1</sup> below the singlet intermediate ( $1IM$ ), predicting a triplet ground state consistent with the experimental observations on  $(\mu-N_2)\{Mo[N(R)Ph]_3\}_2$ . With such a small splitting value, however, a thermal dependence on the measured electronic state would be expected. As a result of the stabilization of the triplet intermediate, the activation energy (measured from  $3IM^*$ ) is calculated to be 107.0 kJ mol<sup>-1</sup> at the UB3LYP/GBS(I) level of theory.

We have carried out further single-point calculations using a triple- $\zeta$  LANL2DZaugmented:6-311+G(2d,p) basis set<sup>67</sup> on the symmetry-broken UB3LYP/GBS(I) geometries. This resulted in only minor changes to the PES, with a small increase in the reaction exothermicity (-252.8 kJ mol<sup>-1</sup>) and energetic shifts of less than 13 kJ mol<sup>-1</sup> for the other species on the reaction

pathway (see the UB3LYP-HL numbers in Table 1). This suggests that LANL2DZ:6-31G(d) provides a good compromise between accuracy and CPU time.

**Density Functional Effects.** Using the nonsymmetry constrained geometries calculated at UB3LYP/GBS(I), we performed single-point calculations on all of the species using a variety of common density functionals (UB3LYP,<sup>26–28</sup> UBLYP,<sup>27,28</sup> UBP86<sup>27,29</sup> and UB3LYP\*<sup>36,43</sup>). The discrepancies observed in the potential energy surfaces resulting from varying the functional are quite significant (Figure 6 and Table 1). The reaction was calculated to be more exothermic by 136 kJ mol<sup>-1</sup> on changing the functional from UB3LYP (-223.8 kJ mol<sup>-1</sup>) to UBP86 (-359.7 kJ mol<sup>-1</sup>). These variations are not due to the use of UB3LYP geometries, as reoptimization with the other functionals does not change the geometries or energetics significantly (the largest change in relative energy arising from reoptimization of the geometries amounts to 2.7 kJ mol<sup>-1</sup>—see Supporting Information). As the DFT functional is varied, similar changes in the relative stability across all of the species is observed, with both the UBP86 and UBLYP density functionals predicting all species to be much more stable relative to reactants than UB3LYP, with the values for UB3LYP\* somewhere in between. While the pure functionals (UBP86 and UBLYP) show a preference for low-spin states, the hybrid functionals (UB3LYP and UB3LYP\*) exhibit a degree of preference for high-spin states.<sup>43</sup>

The variation in the results caused by the choice of density functional creates some uncertainty. While UB3LYP predicts the alternate triplet ( $3IM^*$ ) as the lowest energy intermediate, the other functionals indicate the singlet is lower in energy (Table 1). (Spin density analyses confirmed that all functionals converged to the same singlet and triplet states—see Supporting Information.) Furthermore, the activation energies range from 60.3 (UBP86) to 108.0 kJ mol<sup>-1</sup> (UB3LYP), depending on the choice of functional. Clearly, this is not an ideal situation and in the next section we have used other data to clarify the performance of these density functionals for this system.

**Wave Function Based Methods.** Considering the wide variations in the results from different density functionals and the inability to methodically improve them, we have utilized various wave function methods to systematically explore the effects of electron–electron correlations on the description of this system. As described above, the fundamental difficulty stems from the necessity of describing relative energetics between species with radically different electronic structure due to their varying spin states. Aside from the straightforward comparison between  $4RX+N_2+4RX$  and  $4EC+4RX$ , the formation of all of the species requires at least one electron spin to recouple antiferromagnetically from the reactant species. As will be demonstrated, it is exactly those species with the largest changes in the spin state that prove the most difficult to describe accurately relative to the reactants.

Consider the application of the standard hierarchy of HF, MP2, CCSD, and CCSD(T) to the key species along the reaction pathway, the results of which are presented in Table 1. In general, for complicated transition metal species such as these, the HF approximation lacks the flexibility to even qualitatively describe the energetics, and thus it will not be discussed in any detail. We do note, however, that HF essentially predicts the correct stability of  $4EC+4RX$  relative to the reactants due to the similarities of the two species' electronic structure and their identical spin states. Progressing to MP2 to include a simplistic description of the electronic correlation effects unilaterally stabilizes all of the species, in some cases by hundreds of

**TABLE 1: Variation of the Nitrogen Activation Potential Energy Surface with Changing Theoretical Method (Energies (kJ mol<sup>-1</sup>) Calculated with the GBS(I) Basis Set and UB3LYP/GBS(I) Optimized Geometries)<sup>a</sup>**

	4RX+1N2+4RX	2RX+1N2+4RX	4EC+4RX	2EC+4RX	3IM [3IM*] <sup>b</sup>	1IM	1TS	1PR+1PR	E <sub>act</sub>
UB3LYP	0	56.6	-4.3	-38.5	-141.2 [-154.7]	-152.8	-47.7	-223.8	107.0
UB3LYP-HL <sup>c</sup>	0	58.0	1.0	-26.8	-143.2 [-144.8]	-140.0	-49.5	-252.8	95.3
UBLYP	0	36.0	-4.9	-84.5	-229.0 [-254.4]	-264.2	-195.7	-351.3	68.5
UBP86	0	49.5	-3.6	-89.6	-248.8 [-268.6]	-279.7	-219.4	-359.7	60.3
UB3LYP*	0	51.6	-5.0	-56.2	-177.4 [-193.2]	-195.9	-102.7	-267.7	93.2
HF	0.0	145.0	-1.2	199.1	312.0 [311.2]	430.4	571.3	479.0	260.1
MP2	0.0	119.0	-8.2	67.2	-17.4 [-9.9]	1.4	191.6	-90.2	209.0
	(0.0)	(119.0)	(-8.3)	(66.9)	(-18.4)	(0.5)	(191.6)	(-89.2)	(210.0)
MP2-HL <sup>c</sup>	0.0	114.7	-6.5	42.3	-27.0 [-10.3]	-12.8	140.5	-178.9	167.4
CCSD	0.0	93.4	-7.0	48.5	0.4 [-6.2]	22.9	92.2	-148.0	98.4
	(0.0)	(93.4)	(-7.1)	(48.2)	(-0.6) ([-7.1])	(22.1)		(-147.2)	
CCSD(T)	0.0	74.5	-7.9	17.3	-63.8 [-75.9]	-64.9	1.4	-214.3	77.3
	(0.0)	(74.5)	(-8.0)	(16.9)				(-213.5)	
CCSD(T)-HL <sup>d</sup>	0.0	70.2	-6.2	-7.6	-73.4 [-76.3]	-79.1	-49.7	-303.0	29.4

<sup>a</sup> Those numbers in parentheses refer to full-core (on nitrogen) electron correlation calculations. <sup>b</sup> Square-bracketed terms refer to energies corresponding to the alternate C<sub>1</sub> triplet intermediate geometry (see text). <sup>c</sup> Numbers obtained by carrying out single-point calculations with the large LANL2aug:6-311+G(2d,p) basis set (see Supporting Information). <sup>d</sup> Estimated numbers obtained by adjusting the CCSD(T) values to take into account the basis set effects calculated at the MP2 level.

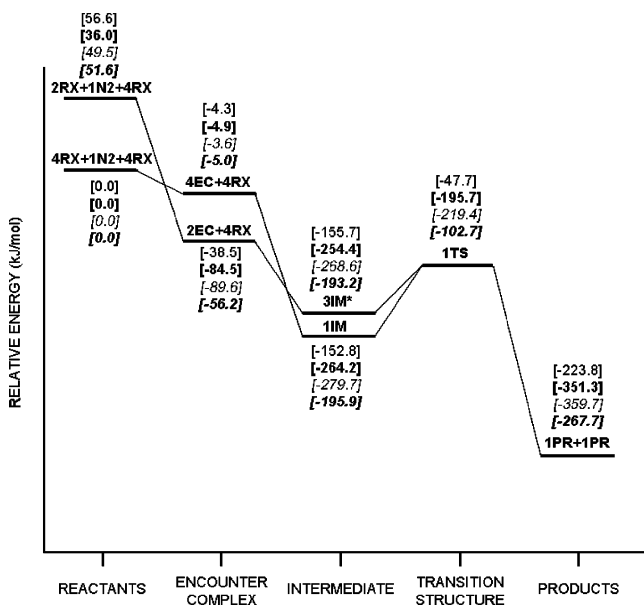


**Figure 6.** Variation of the dinitrogen activation PES with changing density functional. Relative energies are in kilojoules per mole and represent UB3LYP, UBLYP, UB3LYP\*, and UB3LYP\* single-point energies with the GBS(I) basis set on UB3LYP/GBS(I) geometries.

kilojoules per mole when compared to HF. However, given the generally poor quality of the HF description of transition metals, a simple perturbative treatment like MP2 is unlikely to prove adequate. Refinement of the correlation description by CCSD and CCSD(T) generally stabilizes the species substantially, suggesting that a robust description of higher order correlations is important and confirming the inadequacy of MP2. Once again, 4EC+4RX provides an exception to these observations because of its electronic similarity to the reactants. All of the correlated methods predict that the quartet encounter complex lies 7–8 kJ mol<sup>-1</sup> below the quartet reactants.

The results in Table 1 were obtained for the most part with the LANL2DZ:6-31G(d) basis set. To test the adequacy of this basis set, we have also performed MP2 calculations with the triple- $\zeta$  LANL2aug:6-311+G(2d,p) basis set<sup>67</sup> (the results are shown in Table 1 as MP2-HL). This leads to substantial stabilization of 2EC+4RX and 1TS, and an even greater stabilization of 1PR+1PR. If such basis set corrections were transferable to the CCSD and CCSD(T) results (although it has

not been proven rigorously, such an approach has discussed by Quiñero et al.<sup>74</sup>), then it would substantially lower the relative energies. Although it is not practical to do the CCSD(T) calculations with the larger basis set, let alone the more sophisticated methods described below, it must be kept in mind in a discussion of the energies that the wave function based results for 2EC+4RX, 1TS, and 1PR+1PR are almost certainly not converged with respect to basis set and the true relative energies will be somewhat lower.

In the cases where only one spin is flipped from the reactants (i.e. 2RX+1N2+4RX and 2EC+4RX), the steps from MP2 to CCSD and from CCSD to CCSD(T) each stabilize the low-spin species by 20–30 kJ mol<sup>-1</sup>. These low-spin analogues of the quartet reactants and encounter complex have some open-shell character, analogous to going from a triplet diradical to an open-shell singlet diradical, which makes their electronic structure more difficult to determine correctly and helps to explain the importance of the higher order correlations. In the more difficult case of going to the triplet intermediate, which involves the pairing of two sets of spins, the triples effect is even larger at over 60 kJ mol<sup>-1</sup>. The most difficult species to describe relative to the quartet reactants, however, are the singlet state intermediate (1IM), transition structure (1TS), and the products (1PR). In these same cases, we observe very large stabilizations of 20–100 kJ mol<sup>-1</sup> from MP2 to CCSD and an additional 65–90 kJ mol<sup>-1</sup> from CCSD to CCSD(T). Actually, in the cases of 3IM and 1IM, the transition from MP2 to CCSD destabilizes both species slightly, which presumably reflects the overestimation of the doubles by MP2 (neither MP2 nor CCSD is variational). As an internal check on the CCSD wave functions, we have calculated the T<sub>1</sub>-diagnostic<sup>75</sup> for each of the systems in this study (see Supporting Information). Although for the most part these values provide reassurance that the use of the CCSD approach is valid, in a number of cases the results suggest that a closer scrutiny is warranted, as discussed below.

Although the energetic profile suggested by CCSD(T) seems plausible, the large energetic changes between the different levels of model chemistry make it unclear how reliable these results are. To assess the quality of these results, we investigate (1) the ability of CCSD to describe the low-spin species, (2) the orbital effects on the reaction energetics, and (3) the convergence of the higher order correlations.

As mentioned previously, the description of low-spin, open-shell species compared to their high-spin counterparts can be

**TABLE 2: Low-Spin/High-Spin Splittings for the Reactant, Encounter Complex, and Intermediate Species (kJ mol<sup>-1</sup>)<sup>a</sup>**

	RX GAP (2RX–4RX)	EC GAP (2EC–4EC)	IM GAP (1IM–3IM)	IM* GAP (1IM–3IM*)
CCSD	93.4	55.3	22.7	29.2
SF-CCSD	100.3	57.1	28.7	33.3

<sup>a</sup> All results include full-core electron correlation; A positive value indicates a more stable high-spin electronic state.

very difficult due to the increased multiconfigurational character of the low-spin species which can make them difficult to treat with a single reference method such as CCSD. To assess the ability of CCSD to reasonably describe these species, we compute the doublet–quartet and singlet–triplet adiabatic gaps (i.e. from each species' B3LYP-optimized geometry) for four pairs of species, **2RX–4RX**, **2EC–4EC**, **1IM–3IM**, and **1IM–3IM\***, using both CCSD and spin-flip CCSD (see Table 2). In all four cases, SF-CCSD compares well against ordinary CCSD. The differences between the two methods range from 2 kJ mol<sup>-1</sup> (**2EC–4EC**) to 7 kJ mol<sup>-1</sup> (**2RX–4RX**), suggesting that CCSD is sufficiently flexible to capture the dominant features of these different spin states.

Although the SF-CCSD results suggest that CCSD is performing reasonably well (to the extent that a doubles-level treatment may describe the system), it is well-known that wave function instabilities at the HF level that arise from describing a highly correlated system with the mean-field approximation, though not particularly pronounced at the CCSD level, can lead to disastrous predictions at the MP2 or CCSD(T) levels.<sup>44</sup> Therefore, we reexamine the CCSD and CCSD(T) results using OD and OD(T), which reoptimize the orbitals at the CCD level and have been shown to drastically improve upon the HF-orbital results in many symmetry-breaking problems.<sup>54,56</sup> Looking at Table 3, we see that the description from the improved orbitals in OD does not differ much from the CCSD one. This is unsurprising, since CCSD is known to be fairly insensitive to changes in the wave function.<sup>44,68</sup> The largest absolute change at the OD level occurs for the products, which are predicted to be slightly less stable (7 kJ mol<sup>-1</sup>, or 4%) than at the CCSD level. The orbital effects are much more pronounced in OD(T), particularly for the products, due to the increased sensitivity of (T) to instabilities in the HF wave function.<sup>44</sup> Reoptimizing the orbitals with a CCD wave function, which is better able to describe the electronic structure of the singlet products, lowers the reaction energy by 25.5 kJ mol<sup>-1</sup>, or 12%. Again, the doublet-state reactants and encounter complex are not too strongly affected relative to the reactants, suggesting that the orbital effects are relatively small in these cases.

Unfortunately, the added computational expense of OD makes it computationally intractable for the largest species (**3IM**, **1IM**, and **1TS**) in this system. For this reason, we also utilize the low-cost approximations KS-CCSD/KS-CCSD(T), in which Kohn–Sham orbitals from a DFT calculation replace the HF ones in a standard CCSD or CCSD(T) calculation. The results of KS-CCSD/KS-CCSD(T) using either B3LYP or BP86 results agree nicely with each other and with OD/OD(T), differing only by 1–2 kJ mol<sup>-1</sup> for the various species in this system. The fact that the energies resulting from B3LYP, BP86, and OD models disagree substantially, while their orbitals lead to almost identical results at their respective CCSD(T)/OD(T) levels is not at all contradictory. Rather, the improved performance of KS-CCSD(T) or OD(T) depends in large part on the smoothly changing nature of the DFT or OD orbitals in the relevant regions of the potential energy surfaces (i.e. they tend to delay the onset of symmetry breaking to beyond the stationary point

regions of the potential energy surface), rather than on the details of the DFT energetics. How then do the KS-CCSD(T) results compare to CCSD(T) for intermediates and the transition structure? All three intermediate species are lowered by about 15 kJ mol<sup>-1</sup> relative to the reactants, doing little to change their positions relative to one another. The alternate triplet intermediate, **3IM\***, remains the most stable intermediate by ca. 10 kJ mol<sup>-1</sup>, while **3IM** and **1IM** remain very near in energy. On the other hand, KS-CCSD(T) drastically lowers the relative energy of the singlet transition structure, from +1.4 kJ mol<sup>-1</sup> relative to the reactants at the CCSD(T) level to –46.6 kJ mol<sup>-1</sup> at the KS-CCSD(T) level, thereby almost halving the activation barrier. This change will be discussed in more detail below, when the effect of quadruple excitations is analyzed.

Finally, the very large effect of the (T) correction suggests that it is important to gauge the convergence of these results with respect to even higher order correlation effects. In particular, we computed the CCSD(2), OD(2), and KS-CCSD(2) results for as many of the species as possible, and the results are presented in Table 3. The additional expense of the (2) correction versus the (T) one makes it computationally unaffordable for the intermediates and transition structures (except in the case of KS-CCSD(2) for **1TS**, for which the *C*<sub>2h</sub> symmetry of the B3LYP solution makes it feasible). The overall energetic results from the different (2) methods are in good agreement with each other, typically differing by no more than a few percent. The much smaller effect of the different orbitals on the (2) methods as compared to the (T) ones is explained by the generally decreased dependence of (2) on the HF wave function.

The (2) results also are generally similar to those from KS-CCSD(T). To understand these correlation effects better, we break down the relative triple and quadruple correlation effects in (2) across the different species (see Table 4). For the undemanding comparison between the quartet reactants and the quartet encounter complex (i.e. no change in spin state), the triple and quadruple effects are very small and are presumably very well converged. The doublet reactant and encounter complex, which flip one spin relative to the quartet reactants, lead to a more substantial triple effect, typically –15 to +40 kJ mol<sup>-1</sup>, and make a notable difference in the energetics. Fortunately, the quadruple effect for these same species is only around –1 to –5 kJ mol<sup>-1</sup> and the triples-only methods seem to be fairly well converged. These cases do make it clear, however, that the difficulty of describing species with different spin states and vastly different electronic structure requires a high level of correlation for accurate prediction.

The singlet-state products and transition structures, which involve the flipping of three spins relative to the reactants, provide the most troubling cases: the relative triple contributions to the transition structures and the products are –99 and –71 kJ mol<sup>-1</sup>, respectively. Even more dramatic, the relative quadruple effects are –31.4 and –25.0 kJ mol<sup>-1</sup>, perhaps the largest quadruple contributions ever reported! These large higher order correlation effects suggest that an iterative treatment of triples and quadruples or even higher level correlations could still be important for additional accuracy. Unfortunately, such contributions remain extremely expensive to calculate and are beyond feasibility with current techniques in a system of this complexity.

Overall, the (T) and (2) results tend to agree fairly well, despite the addition of quadruple correlation effects in (2). In large part, this similarity may be attributed to the known fact that (T) generally tends to overestimate the triple contribution,<sup>69</sup>



**TABLE 3: Energetic Variation of Selected Species on the Reaction Pathway Using Extended Electron Correlation Methods (kJ mol<sup>-1</sup>)<sup>a</sup> (CCSD and CCSD(T) Results Reprinted Here for Convenience)**

	4RX+1N2+4RX	2RX+1N2+4RX	4EC+ 4RX	2EC+ 4RX	3IM [3IM*]	1IM	1TS	1PR+1PR	<i>E</i> <sub>act</sub>
CCSD	0	93.4	-7.9	48.2	0.4 [-6.2]	22.9	92.2	-147.2	98.4
OD	0	92.2	-7.1	53.5				-140.8	
KS-CCSD <sup>b</sup>	0	93.9	-7.0	56.4	16.5 [10.5]	37.4	110.8	-134.1	144.6
KS-CCSD <sup>c</sup>	0	95.3	-7.0	58.0				-134.2	
CCSD(T)	0	74.5	-8.0	16.9	-63.8 [-75.9]	-64.9	1.4	-213.5	77.3
OD(T)	0	72.1	-7.9	18.3				-239.0	
KS-CCSD(T) <sup>b</sup>	0	72.2	-8.0	15.9	-75.2 [-89.6]	-79.9	-46.6	-240.6	43.0
KS-CCSD(T) <sup>c</sup>	0	71.4	-8.0	15.3				-242.4	
CCSD(2)	0	78.8	-8.0	21.6				-226.6	
OD(2)	0	76.8	-7.9	24.0				-230.9	
KS-CCSD(2) <sup>b</sup>	0	78.0	-7.9	23.6			-19.9	-230.5	69.7 <sup>d</sup>

<sup>a</sup> All results include full-core electron correlation on nitrogen, except for **nIM** and **1TS**, which have frozen nitrogen cores. <sup>b</sup> B3LYP orbitals were used instead of HF orbitals. <sup>c</sup> BP86 orbitals were used instead of HF orbitals. <sup>d</sup> Using the KS-CCSD(T) energy for **3IM\***.

**TABLE 4: Relative Triple and Quadruple Excitation Effects across the Potential Energy Surface (kJ mol<sup>-1</sup>)<sup>a</sup>**

	4RX+ 1N2+ 4RX	2RX+ 1N2+ 4RX	4EC+4R X	2EC+4R X	3IM [3IM*]	1IM	1TS	1PR+ 1PR
CCSD(T) triples	0	-18.9	-0.9	-31.3	-64.2 [-82.1]	-87.8	-90.8	-66.3
CCSD(2) triples	0	-13.5	-0.7	-22.3				-54.9
OD(T) triples	0	-20.2	-0.9	-35.0				-98.2
OD(2) triples	0	-14.1	-0.7	-24.8				-66.3
KS-CCSD(T) triples <sup>b</sup>	0	-16.5	-1.0	-40.5	-80.3 [-100.1]	-117.3	-157.5	-106.5
KS-CCSD(2) triples <sup>b</sup>	0	-14.3	-0.8	-27.6			-99.4	-71.5
CCSD(2) quadruples	0	-1.2	-0.1	-4.2				-24.5
OD(2) quadruples	0	-1.4	-0.1	-4.6				-24.6
KS-CCSD(2) quadruples <sup>b</sup>	0	-1.6	-0.1	-5.2			-31.4	-25.0

<sup>a</sup> All results include full-core electron correlation on nitrogen, except for **nIM** and **1TS**. <sup>b</sup> B3LYP orbitals were used instead of HF ones.

putting it on par with the combined triple and quadruple contribution of (2). For the most orbital-dependent species, the singlet products and transition structure, the (T) triple contribution from the heavily spin-contaminated wave function in CCSD(T) seems to underestimate the higher order correlation effect and destabilizes these species somewhat. Removing the spin contamination in the reference determinant via OD(T) or KS-CCSD(T) noticeably increases the size of the (T) triples (perhaps too much), while the (2) treatment provides a more moderate treatment of the triples. In particular, the extremely large triple effect for **1TS** using KS-CCSD(T) is substantially decreased using KS-CCSD(2), which places the transition structure at -20 kJ mol<sup>-1</sup> relative to the reactants instead of -47 kJ mol<sup>-1</sup>. Though the computation of **3IM\*** with KS-CCSD(2) is unaffordable, by using the KS-CCSD(T) value for that species combined with the KS-CCSD(2) value for the transition structure, one can estimate an activation barrier around 70 kJ mol<sup>-1</sup>.

Combining these results from various electronic structure methods, we can now make some assessment of the quality of our predictions. Certainly any wave function-based description without at least a description of triples correlations is unfit to describe this system. On one hand, given a triples- and/or quadruples-level description, the variations between the various approaches (KS, HF, or OD orbitals and (T) or (2)), do not generally change the qualitative details of the mechanism much. Therefore CCSD(T) may be considered to be the least expensive and most accessible wave function-based model chemistry to be used when studying this system. On the other hand, the activation barrier appears highly sensitive to the orbital choices and perturbative corrections, and the predicted chemical kinetics would depend dramatically on the value obtained for this parameter. Whereas it seems likely that the error bars on our predictions for the reactants and encounter complexes are

probably less than 10 kJ mol<sup>-1</sup> in this basis set (based on the agreement among the different methods and the convergence of the correlation energy), those for the intermediates must be at least 15 kJ mol<sup>-1</sup>. The reaction energy varies by some 25 kJ mol<sup>-1</sup>, depending on the orbitals and perturbative correction used. That value is also the size of the quadruples correlation effect, so the sum of the higher order effects is likely to be comparable and provides a reasonable estimate of the error bars. The even larger fluctuations in the transition structure and the very large quadruples effect (-31 kJ mol<sup>-1</sup>) suggests error bars approaching 45 kJ mol<sup>-1</sup> for the (T) methods. If we accept that KS-CCSD(2) provides a more reasonable account of the higher order correlations, the error bars for the transition structure are closer to 25-30 kJ mol<sup>-1</sup>. Because of the vast electronic differences between the reactants and these singlet species, they are also the species that are least converged with respect to higher order correlation effects—they lack the typical cancellation of errors among the highest-order effects. By taking these estimated errors into account, the best predictions from wave function based theory with the GBS(I) basis set place the reaction enthalpy at ca. -230 ± 35 kJ mol<sup>-1</sup> and the activation energy at ca. 70 ± 45 kJ mol<sup>-1</sup>. Contrast these estimated error bars with those of less than 10 kJ mol<sup>-1</sup> typically expected for CCSD(T) in more standard organic systems, where the electronic structure changes much less across the reaction coordinate. These large error bars, unfortunately, are the natural outcome of comparing species with such extremely different electronic structures. Furthermore, this difficulty is not necessarily limited to wave function methods. To some extent, this problem may explain the wide variations among the different density functionals.

**Hybrid Density Functionals.** Given the wide variation between the different functionals and the wave function based methods, one is tempted to revisit the B3LYP functional, which

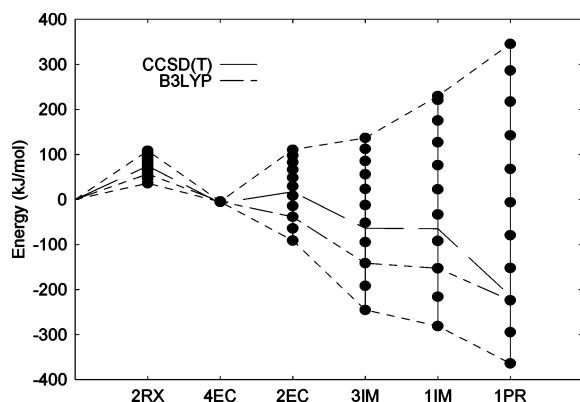


**Figure 7.** Variations in the PES with differing amounts of exact exchange in a B3LYP-like exchange functional relative to the quartet reactants ( $\text{kJ mol}^{-1}$ ). The functional was parametrized as  $E_x = cE_{\text{exact}} + (1 - c)[0.9E_{\text{Becke}} + 0.1E_{\text{Slater}}]$ . Points on the graph mark  $c$  in intervals of 0.1, with smaller values of  $c$  leading to lower energies (except for **4EC**, which due to its similarity to the reactants, depends negligibly on  $c$ ). For comparison, CCSD(T) and B3LYP results are also plotted.

contains three empirical parameters that were fitted using non-transition-metal species. For example, Hess and co-workers have reparametrized the amount of HF (exact) exchange in B3LYP from 0.20 to 0.15 to produce a new functional, B3LYP\*, based on the examination of a few special classes of transition metal complexes.<sup>36,43</sup> However, noting that B3LYP\* is no closer than standard B3LYP in predicting energies comparable to the high-level wave function methods for our system, we have studied the main features of the potential energy surface as a function of the exact exchange admixture, leaving the ratio of the other two exchange components to each other the same (9:1 Becke:Slater exchange), as is presented in Figure 7 (further details are in the Supporting Information). We observe a nearly linear behavior of the energetics as a function of the fraction of HF exchange, which was also observed by Hess and co-workers for species of differing spin states.<sup>36,43</sup> But more importantly, we find a huge variability in the system energetics. The overall reaction varies from 360  $\text{kJ mol}^{-1}$  exothermic (no exact exchange, similar to BLYP) to almost 350  $\text{kJ mol}^{-1}$  endothermic (all exact exchange)—a span of over 700  $\text{kJ mol}^{-1}$ —which leads to completely contradictory and arbitrary chemistry! Moreover, the placement and in some cases even ordering of the various low- and high-spin states varies with the exact exchange admixture. The only species that does not vary significantly with the changes in functional is **4EC**, for which, because of its electronic similarity to **4RX**+**1N<sub>2</sub>**, the variations cancel almost perfectly. Crude linear interpolation suggests that the best agreement with CCSD(T) (chosen as the most affordable representative wave function method), for example, would require HF exchange values of about 0.41 for **2RX**, about 0.35 for **3IM**, and 0.21 for **1PR**. Similarly diverse values would be obtained if one chose any of the other high-level wave function results as a guide. It is possible that this says more about the unreliability of pure HF exchange than the arbitrariness of the mixing coefficient. Given the rapid variation of these energetics with the fraction of HF exchange, no single satisfactory value of this parameter will provide energetics in accord with those calculated with wave function methods over the entire potential energy surface. While this is clearly not an exhaustive analysis of the three-parameter B3LYP functional, it does suggest the challenge inherent in applying modified B3LYP functionals to transition metal systems containing both high- and low-spin states.

### Relevance to the Mechanism for Nitrogen Activation.

Given the energetic differences between CCSD(T) and DFT, is there a danger in trusting the original geometries that were obtained using B3LYP? Reoptimization of the reactants (**4RX** and **2RX**), encounter complexes (**4EC** and **2EC**), and product (**1PR**) using CCSD resulted in the geometries shown in Figure 3 (in bold). These new geometries are in excellent agreement with those obtained via DFT and suggest that our discussion can be restricted to the variation in energies only. For those species on the pathway having low- and high-spin states proximal in energy, CCSD(T) predicts that the high-spin reactant, encounter complex, and intermediate are more stabilized than their respective low-spin species. The calculation of a quartet ground state for the reactant (stabilized by 74.5  $\text{kJ mol}^{-1}$  with respect to the doublet reactant) agrees with both the DFT calculations performed by ourselves and others,<sup>17,21–23</sup> and experimental evidence obtained by Cummins and co-workers.<sup>13</sup> The ground state of the intermediate is predicted at the CCSD(T) level to be a triplet, containing a slightly bent core and a rotated amide group on each of the molybdenum centers. This structure lies 75.9  $\text{kJ mol}^{-1}$  below the energy of reactants and is ca. 10  $\text{kJ mol}^{-1}$  lower in energy than both the pseudo- $S_6$  symmetric triplet (**3IM**) and  $C_1$  symmetric singlet (**1IM**) intermediates. The relatively small separation between these species confirms the importance of the singlet intermediate in the reaction,<sup>23</sup> and in fact application of a larger basis set could lead to a reordering of the states. It is unknown whether the calculated order of states will be transferable to the real system, however, with larger ligands possibly preventing an orientation of amide groups similar to **3IM**\*. Initial QM/MM results on the real system, however, confirm that intermediates bearing rotated amide groups are slightly more energetically favorable than the nonrotated structures,<sup>70</sup> and further calculations being undertaken at QM/QM level are expected to reinforce this.

There is quite a large variation in the doublet–quartet splitting for the encounter complex as calculated with the B3LYP (34.2  $\text{kJ mol}^{-1}$ ) and BP86 (86.0  $\text{kJ mol}^{-1}$ ) functionals. In the experimental system,  $\text{Mo}(\text{N}[\text{R}]\text{Ar})_3$  is found to bind nitrogen very weakly and the encounter complex is not observed, thus restricting any definitive characterization of the electronic state. While nitrogen bound encounter complexes of “Schrock-type” Mo(III) species have been observed and characterized as doublets,<sup>71</sup> the fact that these species bind nitrogen strongly and are experimentally isolable (as stable solids!) suggests a different mechanism may be acting in comparison to the Laplaza and Cummins case. The existence of a doublet encounter complex in the Laplaza and Cummins case is still postulated, however,<sup>72</sup> as increased nitrogen uptake is observed when the reactant is converted from a quartet to a doublet (through ligation of appropriate adducts), possibly as a result of removing the spin flip barrier that exists on going from the quartet reactant to the doublet encounter complex.

The DFT results are consistent with the generally accepted mechanism for the cleavage of the dinitrogen bond by  $\text{MoL}_3$  complexes.<sup>17</sup> In this mechanism the  $\text{MoL}_3$  reactant starts off on the quartet surface, the dinitrogen approaches and (possibly) forms a very weakly bound **4EC**, which then undergoes a spin-flip to form the more strongly bound **2EC**. As discussed by Harvey,<sup>24</sup> this spin flip is associated with a barrier of ca. 30  $\text{kJ mol}^{-1}$  relative to the reactants (Figure 8). The subsequent step of the reaction in which a second quartet  $\text{MoL}_3$  reactant binds to **2EC** to form **3IM** is spin-allowed and is expected to proceed without a barrier.



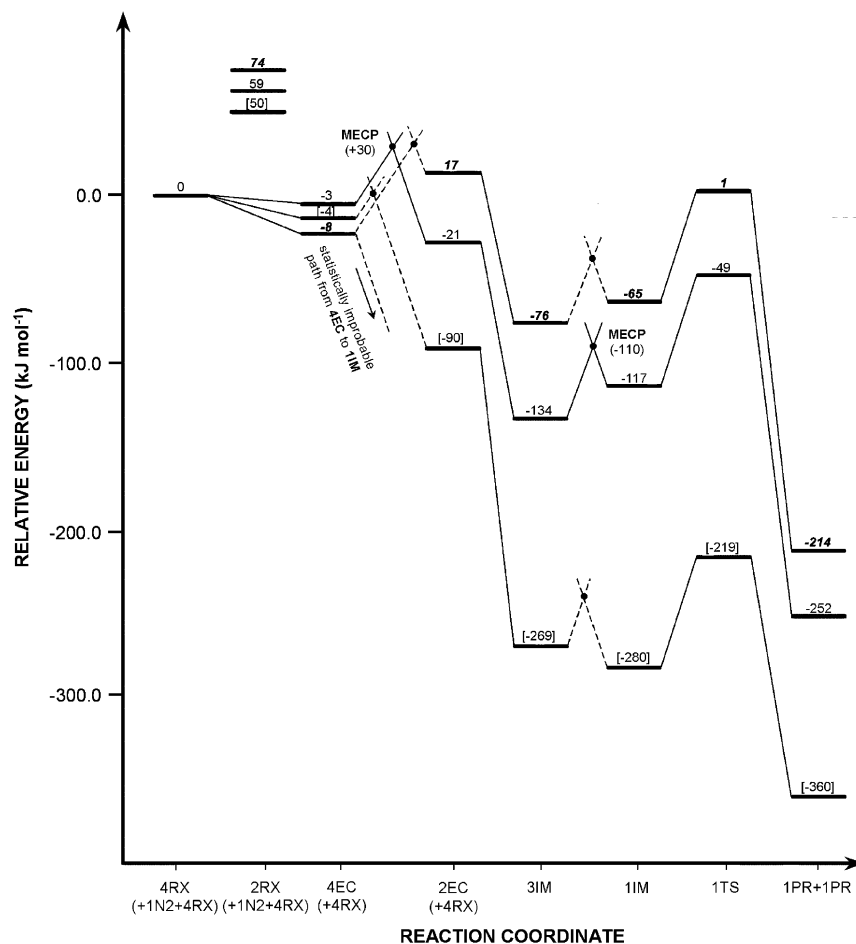


**Figure 8.** Comparison of three different potential energy surfaces for the activation of nitrogen by  $\text{Mo}(\text{NH}_2)_3$ . Results shown are B3LYP/LACV3P: 6-31G(d) (normal typeface) (taken from ref 24 and is almost identical to our B3LYP/GBS(I) calculated numbers), CCSD(T)/GBS(I) (italics) and BP86/GBS(I) (bracketed) (to represent the pure density functional case). Solid dots over dashed connecting lines represent minimum energy crossing points (MECPs) that have not been located.

As mentioned earlier, with larger basis sets it is likely that the CCSD(T) relative energies (Figure 8) will drop and approach those of B3LYP. But even if one assumes that the MP2 basis set shift (MP2-HL–MP2 from Table 1) can be applied to CCSD(T) in a transferable manner, it would still lead to some significant differences compared to DFT. For example, the encounter complexes **4EC** and **2EC** would be nearly isoenergetic at the CCSD(T)-HL level of theory. Under these circumstances, how likely is it for the spin crossing from **4EC** to **2EC** to occur? Superficially there is not much difference in the shapes of the potential energy surfaces drawn in Figure 8, but at the CCSD(T) level there is no driving force to form **2EC** as there is in the DFT mechanism. Nevertheless a consideration of the geometries of **4EC** and **2EC** suggests that as the Mo–N distance in **4EC** becomes shorter, it must at some stage lie higher in energy at the CCSD(T) level than the corresponding doublet structure at the same geometry. There will be a minimum energy crossing point (MECP) for this process, shown as the dashed line between the CCSD(T) values for **4EC** and **2EC** in Figure 8. If the value of this MECP was approximately  $30 \text{ kJ mol}^{-1}$ , then the CCSD(T) and B3LYP mechanisms become coincident. Calculations at the CCSD(T) level are in progress to determine the approximate value of this MECP.

It is important to note that observed trends from calculations on the model system may not extrapolate well to the much larger experimental system. As previously mentioned, amide ligand rotation may well be restricted in the experimental system or the excised substituents may play an important electronic role

in deciding the most stable electronic states. Extension of the model toward the real system presents a significant challenge if we wish to retain the chemical accuracy afforded by CCSD(T) or any of the other higher order methods. Clearly, even application of CCSD(T) to the full system is unrealistic, and as a consequence our subsequent calculations<sup>73</sup> have relied on the ONIOM method with a coupled-cluster high level to predict energetic trends on the real system.

## Conclusions

On undertaking a comprehensive examination of the nitrogen activation potential energy surface, we have found that the reported literature variations primarily result from the choice of density functional employed for the calculations. While careful consideration of the basis-set and optimization constraints resulted in the location of new low-energy structures and validation of the singlet rotated amide intermediate previously described by Stranger's group,<sup>23</sup> the characterization of the electronic ground state for the intermediate was found to be highly sensitive to the choice of density functional. In fact, the relative energies of both the intermediates and products were found to change by more than  $100 \text{ kJ mol}^{-1}$  on going from UB3LYP- to UB86-based calculations. Whenever the description of the system varies this dramatically with different density functionals, one ought to look for external validation to resolve the conflicting data.

In an attempt to obtain a more stable description of the system, we moved to wave function based methods and found

higher order correlations (triple and to some extent quadruple excitations) to be extremely important and that KS-CCSD(T) or CCSD(T) methods are the least expensive approximations that provide reasonable results based on indicators arising from OD, SF-CCSD, and CCSD(2) calculations. Attempts to apply a suitable reparametrized density functional to the system which resulted in energies similar to that obtained with CCSD(T) proved unfeasible, with the energies of the low-spin/high-spin species on the pathway found to be sensitive to the exact Hartree–Fock exchange admixture in the functional to different degrees. As a consequence, great care must be exercised when using density functional theory for this system and similar difficulties may well transfer to comparable systems.

An interpretation of the CCSD(T) results for the reaction reveals a potential energy surface that qualitatively agrees almost exactly with that predicted via B3LYP. The primary discrepancy lies in the prediction of a quartet ground state for the encounter complex; however, the reaction is still likely to proceed via the more tightly bound doublet, which is energetically accessible.

**Acknowledgment.** D.C.G., G.C., R.S., and B.F.Y. would like to thank the Australian Research Council (ARC) for project funding. We are also indebted to the Australian Partnership for Advanced Computing (APAC) for a generous time grant on their parallel computing facility. G.J.O.B and M.H.-G. would like to thank DOE Computational Nanosciences for financial support. G.J.O.B. would also like to thank Prof. A. Krylov for her help with the spin-flip calculations.

**Supporting Information Available:** Computational details for all structures (Cartesian coordinates, energies, and the number of imaginary frequencies) and description of the LANL2DZaugmented:6-311+G(2d,p) basis set (PDF). This material is available free of charge via the Internet at <http://pubs.acs.org>.

## References and Notes

- Burgess, B. K.; Lowe, D. J. *Chem. Rev.* **1996**, *96*, 2983–3011.
- Howard, J. B.; Rees, D. C. *Chem. Rev.* **1996**, *96*, 2965–2982.
- Leigh, G. J. *Science* **1998**, *279*, 506–507.
- Hidai, M. *Coord. Chem. Rev.* **1999**, *186*, 99–108.
- Fryzuk, M. D.; Johnson, S. A. *Coord. Chem. Rev.* **2000**, *200*, 379–409.
- Hidai, M.; Mizobe, Y. *Pure Appl. Chem.* **2001**, *73*, 261–263.
- Schrock, R. R. *Chem. Commun.* **2003**, 2389–2391.
- Fryzuk, M. D. *Chem. Rec.* **2003**, *3*, 2–11.
- Shaver, M. P.; Fryzuk, M. D. *Adv. Synth. Catal.* **2003**, *345*, 1061–1076.
- MacKay, B. A.; Fryzuk, M. D. *Chem. Rev.* **2004**, *104*, 385–401.
- Laplaza, C. E.; Cummins, C. C. *Science* **1995**, *268*, 861–863.
- Laplaza, C. E.; Davis, W. M.; Cummins, C. C. *Angew. Chem., Int. Ed. Engl.* **1995**, *34*, 2042–2044.
- Laplaza, C. E.; Johnson, M. J. A.; Peters, J. C.; Odom, A. L.; Kim, E.; Cummins, C. C.; George, G. N.; Pickering, I. J. *J. Am. Chem. Soc.* **1996**, *118*, 8623–8638.
- Cummins, C. C. *Chem. Commun.* **1998**, 1777–1786.
- Laplaza, C. E.; Odom, A. L.; Davis, W. M.; Cummins, C. C.; Protasiewicz, J. D. *J. Am. Chem. Soc.* **1998**, *120*, 4999–5000.
- Predictions based on Raman spectral data estimate the N–N bond length in the same complex to be 1.23 Å.
- Cui, Q.; Musaev, D. G.; Svensson, M.; Sieber, S.; Morokuma, K. *J. Am. Chem. Soc.* **1995**, *117*, 12366–12367.
- Neyman, K. M.; Nasluzov, V. A.; Hahn, J.; Landis, C. R.; Rosch, N. *Organometallics* **1997**, *16*, 995–1000.
- Hahn, J.; Landis, C. R.; Nasluzov, V. A.; Neyman, K. M.; Rosch, N. *Inorg. Chem.* **1997**, *36*, 3947–3951.
- Johnson, A. R.; Davis, W. M.; Cummins, C. C.; Serron, S.; Nolan, S. P.; Musaev, D. G.; Morokuma, K. *J. Am. Chem. Soc.* **1998**, *120*, 2071–2085.
- Khoroshun, D. V.; Musaev, D. G.; Morokuma, K. *Organometallics* **1999**, *18*, 5653–5660.
- Khoroshun, D. V.; Musaev, D. G.; Morokuma, K. *Mol. Phys.* **2002**, *100*, 523–532.
- Christian, G.; Driver, J.; Stranger, R. *Faraday Discuss.* **2003**, *124*, 331–341.
- Roos, B. O.; Siegbahn, P. E. M.; Eisenstein, O.; Perutz, R. N.; McGrady, G. S.; Deeth, R. J.; Bandeira, N. A. G.; Green, J. C.; Meuwly, M.; Harvey, J. N.; Drummond, M. L.; Jensen, K. P.; Richardson, N. A.; Frenking, G.; Bursten, B. E.; Schaefer, H. F.; Hay, P. J.; Costuas, K.; Christian, G.; Stranger, R.; Kaltsosyannis, N.; Meier, R. J.; Ziegler, T. *Faraday Discuss.* **2003**, *124*, 343–352.
- Cherry, J. P. F.; Johnson, A. R.; Baraldo, L. M.; Tsai, Y. C.; Cummins, C. C.; Kryatov, S. V.; Rybak-Akimova, E. V.; Capps, K. B.; Hoff, C. D.; Haar, C. M.; Nolan, S. P. *J. Am. Chem. Soc.* **2001**, *123*, 7271–7286.
- Becke, A. D. *J. Chem. Phys.* **1993**, *98*, 5648–5652.
- Becke, A. D. *Phys. Rev. A* **1988**, *38*, 3098–3100.
- Lee, C.; Yang, W.; Parr, R. G. *Phys. Rev. B* **1988**, *37*, 785–789.
- Perdew, J. P. *Phys. Rev. B* **1986**, *33*, 8822–8824.
- Ziegler, T. *Chem. Rev.* **1991**, *91*, 651–667.
- Eriksson, L. A.; Pettersson, L. G. M.; Siegbahn, P. E. M.; Wahlgren, U. *J. Chem. Phys.* **1995**, *102*, 872–878.
- Ricca, A.; Bauschlicher, C. W. *Theor. Chim. Acta* **1995**, *92*, 123–131.
- Siegbahn, P. E. M. *Adv. Chem. Phys.* **1996**, *93*, 333–387.
- Torrent, M.; Sola, M.; Frenking, G. *Chem. Rev.* **2000**, *100*, 439–493.
- Niu, S. Q.; Hall, M. B. *Chem. Rev.* **2000**, *100*, 353–405.
- Reiher, M.; Salomon, O.; Hess, B. A. *Theor. Chem. Acc.* **2001**, *107*, 48–55.
- Khoroshun, D. V.; Musaev, D. G.; Vreven, T.; Morokuma, K. *Organometallics* **2001**, *20*, 2007–2026.
- Khavrutskii, I. V.; Musaev, D. G.; Morokuma, K. *Inorg. Chem.* **2003**, *42*, 2606–2621.
- Cavallo, L.; Jacobsen, H. J. *Phys. Chem. A* **2003**, *107*, 5466–5471.
- Khavrutskii, I. V.; Musaev, D. G.; Morokuma, K. *J. Am. Chem. Soc.* **2003**, *125*, 13879–13889.
- Khavrutskii, I. V.; Rahim, R. R.; Musaev, D. G.; Morokuma, K. *J. Phys. Chem. B* **2004**, *108*, 3845–3854.
- Jacobsen, H.; Cavallo, L. *Phys. Chem. Chem. Phys.* **2004**, *6*, 3747–3753.
- Salomon, O.; Reiher, M.; Hess, B. A. *J. Chem. Phys.* **2002**, *117*, 4729–4737.
- Crawford, T. D.; Stanton, J. F.; Allen, W. D.; Schaefer, H. F. J. *Chem. Phys.* **1997**, *107*, 10626–10632.
- Dunietz, B. D.; Head-Gordon, M. *J. Phys. Chem. A* **2003**, *107*, 9160–9167.
- Byrd, E. F. C.; Sherrill, C. D.; Head-Gordon, M. *J. Phys. Chem. A* **2001**, *105*, 9736–9747.
- Barnes, L. A.; Lindh, R. *Chem. Phys. Lett.* **1994**, *223*, 207–214.
- Jensen, F. *Chem. Phys. Lett.* **1990**, *169*, 519–528.
- Sherrill, C. D.; Lee, M. S.; Head-Gordon, M. *Chem. Phys. Lett.* **1999**, *302*, 425–430.
- Cohen, R. D.; Sherrill, C. D. *J. Chem. Phys.* **2001**, *114*, 8257–8269.
- Møller, C.; Plesset, M. S. *Phys. Rev.* **1934**, *46*, 618.
- Purvis, G. D., III; Bartlett, R. J. *J. Chem. Phys.* **1982**, *76*, 1910–1918.
- Raghavachari, K.; Trucks, G. W.; Pople, J. A.; Head-Gordon, M. *Chem. Phys. Lett.* **1989**, *157*, 479–483.
- Sherrill, C. D.; Krylov, A. I.; Byrd, E. F. C.; Head-Gordon, M. *J. Chem. Phys.* **1998**, *109*, 4171–4181.
- Chiles, R. A.; Dykstra, C. E. *J. Chem. Phys.* **1981**, *74*, 4544.
- Beran, G. J. O.; Gwaltney, S. R.; Head-Gordon, M. *Phys. Chem. Chem. Phys.* **2003**, *5*, 2488–2493.
- Gwaltney, S. R.; Head-Gordon, M. *Chem. Phys. Lett.* **2000**, *323*, 21–28.
- Gwaltney, S. R.; Head-Gordon, M. *J. Chem. Phys.* **2001**, *115*, 2014–2021.
- Krylov, A. I. *Chem. Phys. Lett.* **2001**, *338*, 375–384.
- Levchenko, S. V.; Krylov, A. I. *J. Chem. Phys.* **2004**, *120*, 175–185.
- Slipchenko, L. V.; Krylov, A. I. *J. Chem. Phys.* **2002**, *117*, 4694–4708.
- Frisch, M. J.; Trucks, G. W.; Schlegel, H. B.; Scuseria, G. E.; Robb, M. A.; Cheeseman, J. R.; Montgomery, J. A., Jr.; Vreven, T.; Kudin, K. N.; Burant, J. C.; Millam, J. M.; Iyengar, S. S.; Tomasi, J.; Barone, V.; Mennucci, B.; Cossi, M.; Scalmani, G.; Rega, N.; Petersson, G. A.; Nakatsuji, H.; Hada, M.; Ehara, M.; Toyota, K.; Fukuda, R.; Hasegawa, J.; Ishida, M.; Nakajima, T.; Honda, Y.; Kitao, O.; Nakai, H.; Klene, M.; Li, X.; Knox, J. E.; Hratchian, H. P.; Cross, J. B.; Adamo, C.; Jaramillo, J.; Gomperts, R.; Stratmann, R. E.; Yazyev, O.; Austin, A. J.; Cammi, R.; Pomelli, C.; Ochterski, J. W.; Ayala, P. Y.; Morokuma, K.; Voth, G. A.; Salvador, P.; Dannenberg, J. J.; Zakrzewski, V. G.; Dapprich, S.; Daniels,

- A. D.; Strain, M. C.; Farkas, O.; Malick, D. K.; Rabuck, A. D.; Raghavachari, K.; Foresman, J. B.; Ortiz, J. V.; Cui, Q.; Baboul, A. G.; Clifford, S.; Cioslowski, J.; Stefanov, B. B.; Liu, G.; Liashenko, A.; Piskorz, P.; Komaromi, I.; Martin, R. L.; Fox, D. J.; Keith, T.; Al-Laham, M. A.; Peng, C. Y.; Nanayakkara, A.; Challacombe, M.; Gill, P. M. W.; Johnson, B.; Chen, W.; Wong, M. W.; Gonzalez, C.; Pople, J. A., *Gaussian 03*, Revision B.05; Gaussian, Inc.: Pittsburgh, PA, 2003
- (63) Kong, J.; White, C. A.; Krylov, A. I.; Sherrill, D.; Adamson, R. D.; Furlani, T. R.; Lee, M. S.; Lee, A. M.; Gwaltney, S. R.; Adams, T. R.; Ochsenfeld, C.; Gilbert, A. T. B.; Kedziora, G. S.; Rassolov, V. A.; Maurice, D. R.; Nair, N.; Shao, Y. H.; Besley, N. A.; Maslen, P. E.; Dombroski, J. P.; Daschel, H.; Zhang, W. M.; Korambath, P. P.; Baker, J.; Byrd, E. F. C.; Van Voorhis, T.; Oumi, M.; Hirata, S.; Hsu, C. P.; Ishikawa, N.; Florian, J.; Warshel, A.; Johnson, B. G.; Gill, P. M. W.; Head-Gordon, M.; Pople, J. A. *J. Comput. Chem.* **2000**, *21*, 1532–1548.
- (64) Dunning, T. H.; Hay, P. J. *Modern Theoretical Chemistry*; Plenum: New York, 1976; Vol. 3.
- (65) Hay, P. J.; Wadt, W. R. *J. Chem. Phys.* **1985**, *82*, 299.
- (66) Hariharan, P. C.; Pople, J. A. *Theor. Chim. Acta* **1973**, *28*, 213–222.
- (67) Incorporating the LANL2 ECP, uncontracted and well-tempered extensions to the s-, p-, and d-functions of LANL2DZ along with an even scaling rule extension of the f-function recommended by Frenking and co-workers (Ehlers, A. W.; Bohme, M.; Dapprich, S.; Gobbi, A.; Hollwarth, A.; Jonas, V.; Kohler, K. F.; Stegmann, R.; Veldkamp, A.; Frenking, G. *Chem. Phys. Lett.* **1993**, *208*, 111–114) on molybdenum and the 6-311+G-(2d,p) basis set on all other atoms. The complete basis set can be found in the Supporting Information.
- (68) Salter, E. A.; Sekino, H.; Bartlett, R. J. *J. Chem. Phys.* **1987**, *87*, 502–509.
- (69) Ruden, T. A.; Helgaker, T.; Jørgensen, P.; Olsen, J. *J. Chem. Phys.* **2004**, *121*, 5874–5884.
- (70) Christian, G.; Stranger, R.; Graham, D. C.; Yates, B. F. *Dalton Trans.* **2005**, *5*, 962–968.
- (71) O'Donoghue, M. B.; Zanetti, N. C.; Davis, W. M.; Schrock, R. R. *J. Am. Chem. Soc.* **1997**, *119*, 2753–2754.
- (72) Tsai, Y. C.; Cummins, C. C. *Inorg. Chim. Acta* **2003**, *345*, 63–69.
- (73) Graham, D. C.; Yates, B. F.; Stranger, R.; Christian, G. Manuscript in preparation.
- (74) Quiñonero, D.; Musaev, D. G.; Morokuma, K. *Inorg. Chem.* **2003**, *42*, 8449–8455.
- (75) Lee, T. J.; Taylor, P. R. *Int. J. Quantum Chem., Quantum Chem. Symp.* **1989**, *23*, 199–207.